Research on Control Method and Evaluation System of Ground Unmanned Vehicle Formation Transform

Tianyu Shi [1,2] ,Zhichao Wang[1,2],Chong hao Zou[1,2],Sunbo Wang[3],Yunqing Bao,Shihua Yuan[1]*,Xueyuan Li[1]*, Junjie Zhou[1]

Abstract

In this paper, we design a formation control system for unmanned ground vehicles (UGV) from the perspective of path planning and path tracking. The master-slave control is adopted by electing out a main vehicle to address the problem of possible accumulation, transmission and amplification of errors. In the process of formation transformation, we first generate an expected path by combining the methods of dynamic window and potential energy field. Then a path tracking algorithm based on Hermite curve is adopted to make the formation transformation process more stable and accurate. Finally, the evaluation system of the formation control system is constructed, which combines the expected position, the actual position, the expected speed, the actual speed and the actual acceleration, giving an evaluation on the performance of the formation transformation，response of the formation driving process and the performance of the formation stability.

Keywords

Unmanned ground vehicle, swarms, formation control, path tracking, stability analysis

Introduction

Generally, UGVs are driven by electric or hydraulic power. Differential steering is used to provide different speeds for the wheels on the left and right sides of the wheel, which results in the speed difference and realizes sliding steering on the ground. [12]. The steering characteristics of a vehicle with differential steering are difficult to accurately describe because of the extremely complex motion and the force between the wheels and the ground. [9] In this paper, it is adopted a commonly used 4×4 UGV as our research object and build the dynamic model based on guidance track concept [10], which can reduce the inaccuracy problem and control parameters.

Presently, the typical formation control method mainly includes leader follow law [12], virtual structure law [13] and behavior-based law [14]. Our essential control ideology based on a concept of voting leader follow method which is a combination of centralized and decentralized formation control method [15] and can maintain better and steadier formation moving and reduce the calculation complexity. The whole behavior of the system is decomposed into some basic and simple sub-behaviors, which includes path planning, path tracking, and formation maintaining. Firstly, these operations are relatively independent; secondly, each child behavior has a corresponding behavior. And first, for the path planning level [1], the essence is how to reach the target position from its location [1], in the formation transformation process, not only need to consider how the fastest and shortest distance to reach the destination, but also need to consider how to avoid collision with other vehicles during formation. The artificial potential field method (APF) [2]is mainly used in the robot path planning problem, but it does not take the relative motion problem of the surrounding dynamic obstacles into account. In this paper, we have considered the related motion disturbance in formation process, and combine the dynamic window approach (DWA) [3]to consider the vehicle's motion performance synthetically, and search out the optimal change team path in a certain area, which makes the formation transformation more safe and efficient.

And for the unmanned vehicle path tracking level, the accuracy and stability of its tracking are mainly considered. The stability can be better maintained by the modified Liapunov function control [17]. At the same time, the Liapunov function also has better stability in the tracking control of industrial robots [5]. The path tracking method for 4×4 UGV deduced in this paper adopts the parametric curve approximation method to control the approaching curve through the speed and direction of the vehicle's two points, so that the vehicle can align the head direction during the path tracking process. In addition, the speed and yaw rate are used for input tracking according to the situation targeted by the article.

Our contributions are

1. Presenting a modified APF with DWA based model which can mitigate the disturbance of moving obstacles and can make the formation process more adaptable to vehicle performance and can help the process to be safer and more efficient.
2. Presenting a time-series-based unmanned vehicle path tracking algorithm, setting the parameters such as vehicle speed and yaw rate as parameter equations with time as independent variables, and embodying the control quantity in discrete time.
3. Presenting a rational equation to evaluate the performance of the following process which can help modify the parameter

The rest of paper is organized as follows, in the following section, the kinematics properties of the differential steering vehicle model are illustrated. The third section discusses two level of control algorithm from path planning and following. Then simulations are provided to show the effectiveness of the proposed method and a evaluation system is established to analyze the results. Finally, this paper is then concluded in the final section.

[1.] National key laboratory of vehicular transmission, Beijing Institute of Technology, Beijing ,100081, China
[2.]Ground-Aerial Intelligent Vehicle Joint laboratory, Beijing Institute of Technology, Beijing ,100081, China
[3.]School of Automation, Beijing Institute of Technology, Beijing, 100081, China
[4.]School of Electronics and Information, Beijing Institute of Technology, Beijing, 100081, China

L	the width between the left and right axles (It means the width between the left and right wheels)
d	wheel diameter,
v_c	the speed of the centroid of the vehicle,
w_c	yaw rate for the vehicle,
R_C	turning radius for the vehicle (the distance from the turning center to the centroid of the vehicle)
v_L / v_R	left and right wheel speeds
θ_0	the initial turning angle of the vehicle
v_c, w_c	the current speed of the unmanned vehicle
$\dot{v_a}$, $\dot{v_d}$	the maximum heading acceleration and deceleration of the unmanned vehicle
$\dot{w_d}$ $\dot{w_a}$	the largest yaw angular acceleration and deceleration of the unmanned vehicle
U_r	the repulsive potential field
U_a	the gravitational potential field
ρ_0	the detection range of the vehicle
ρ_i	radius of the repulsion circle centered on the ith obstacle in the detection range
v_{max}	the maximum relative speed of the obstacle and the vehicle
v'	the current speed of the obstacle pointing vehicle
ρ_r	the specified radius value selected according to the obstacle and vehicle attributes
target	
K	the gain constant,
v	the current speed of the vehicle
v_{goal}	the target moving speed
v_{obs}	the moving obstacle speed, q is the vehicle position loss
q_{goal}	the target vector
q_{obs}	the moving obstacle position vector,
ρ	the distance between the vehicle and the obstacle
s(t)	the actual position of the vehicle
$s_{ideal}(t)$	expected position of the vehicle
a(t)	the instantaneous acceleration of the vehicle
e_x'	the unit vector of x-axis

Vehicle Model Formulation

Unmanned vehicle kinematics model

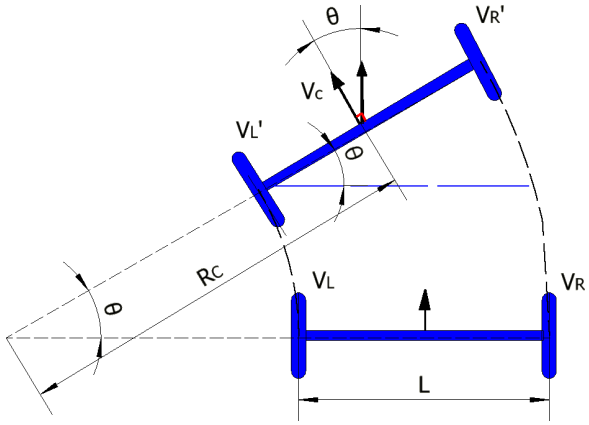

Fig.1. 4x4 unmanned vehicle dynamics model

In order to simplify the model, only the following driving wheels are considered as the research object in this paper, so it can be simplified as a two-wheeler model, assuming that the wheels of the ground unmanned vehicle move on a flat horizontal ground, and the wheels only have rolling contact with the ground, according to its geometry relationship, the vehicle kinematics model can be built as follows:

$$V = [v_L\ v_R] = \left[w_c \times \left(R_c - \frac{L}{2}\right)\ \ w_c \times \left(R_c + \frac{L}{2}\right)\right] \quad (1)$$

The unmanned vehicle steers according to the speed difference between the left and right wheels. When the unmanned vehicle is in motion along a straight line , since the R tends to be infinite, the four-wheel speeds of the unmanned vehicle are equal, which is, $v_L = v_R$. When the unmanned vehicle performs a retreating motion, we need only reverse the rotation speed of all the wheels of the vehicle. If performing an in-place rotation motion, due to R=0 and v_c=0, so $v_L = -v_R$. The vehicle adopts four-wheel differential steering system and the control method is simple. However, since the wheels cannot rotate freely, making the motion freedom of the unmanned vehicle low, so a large steering circle space is needed during the turning process, which means that there need a threshold to limit the steering speed and the yaw rate so that the vehicle will be steadily controlled and the mutual interference between the vehicles can be avoided.

Track deduction is an idea for the bottom control of the robot, which is based on the unmanned vehicle posture (position, posture) and then calculates the speed and yaw rate of unmanned vehicle, and the speeds of left and right wheel. Conversely, it is also possible to reverse the attitude parameters based on the vehicle speed parameters.

First, according to the geometric relations, $\theta_1 = \theta_2 = \theta_3$ can be obtained. The driving wheel of the vehicle is selected as the research object. Because there are two speeds, the vehicle model is a two-degree-of-freedom model. From this, we establish a time-dependent equation to establish a track derivation model. Considering the relative speed relationship between the left and

right wheel and the body width L, the yaw rate of an unmanned vehicle can be expressed as:

$$\frac{d\theta}{dt} = \frac{(v_R - v_L)}{L} \tag{2}$$

By integrating, we can get the vehicle corner:

$$\theta = \frac{(v_R - v_L)t}{L} + \theta_0 \tag{3}$$

Similarly, the moving speed of the vehicle can be calculated as:

$$v_c = \frac{(v_R + v_L)}{2} \tag{4}$$

Through sophisticated consideration of the forward velocity and yaw rate of the vehicle, multiple sets of motion parameters are generated by local path planning, and thereafter the trajectory can be deduced by integrating the speed.

$$\begin{cases} x(t_n) = x(t_0) + \int_{t_0}^{t_n} v_{c(t)} cos\theta(t) dt \\ y(t_n) = y(t_0) + \int_{t_0}^{t_n} v_{c(t)} sin\theta(t) dt \end{cases} \tag{5}$$

Control Algorithms

Overall formation transformation

For the formation transformation, here presupposes that five vehicles make up a team. The initial formation is longitudinally arranged, which is transformed into a horizontal line, a triangular line, and finally a longitudinal line. The detailed process is as follows:

The vehicles of the initial fleet are numbered 1-5, and number 3 is in the middle position, which is determined as the main vehicle. When changing the formation, the baseline of the path of the other four vehicles is obtained by shifting the baseline of the path of the main vehicle to the left and right, corresponding to No. 1, No. 2, No. 4 and No. 5. Each vehicle is planning an expected path and reaching the target baseline along the expected path. At the same time, each one adjusts the speed to ensure the positions of the vehicle is accurately aligned, and then completes the transformation from the longitudinal line to the horizontal line.

When the formation converts to a triangle line, it only needs to change the speed in turn, No. 1 and No. 5 at low speed, No. 2 and No. 4 at medium speed, and No. 5 at high speed. After pulling away the distance, the triangle formation is converted.

The above is a complete formation transformation process. When the formation is restored, the reverse process of the above process is adopted.

The determination of the main vehicle: For the whole formation transformation process, like the longitudinal line converts to the oblique line, the oblique line converts to horizontal line, and the horizontal line converts to the triangular line, the No. 3 main vehicle always keeps a straight line along the road, all the paths of subordinate vehicles are obtained on the basis of the path of the main vehicle, and the position of all the subordinate vehicles is relatively balanced with respect to the main vehicle to ensure that the main vehicle is located in the center of the team. Therefore, at the beginning of the formation, set No. 3 as the main vehicle and use it as the basis for the formation transformation.

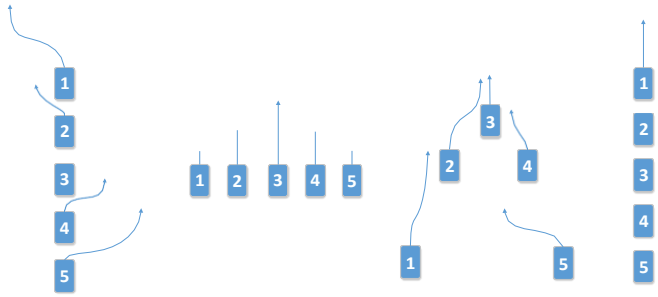

Fig.2. Formation transformation Diagram

Path Planning

Path planning is to deduct the next state parameter (v_{t+1}, w_{t+1}) in accordance with the motion parameters (v_t, w_t) of the unmanned vehicle at the previous moment. Based on the previously constructed vehicle trajectory estimation formula（5）, the trajectory can be deduced from the velocity, because of taking into account the computational complexity , when sampling on an unmanned vehicle in motion, only sampling multiple sets of velocity parameters (v, w) in two-dimensional space. The velocity parameter (v, w) can thereafter be used to extrapolate the trajectory of the vehicle.

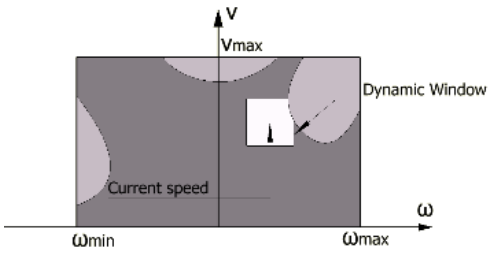

Fig.3. sketch map of dynamic window

First , unmanned vehicles are limited by their own maximum speed and minimum speed:

$$V_m = \{v \in [v_{min}, v_{max}], w \in [w_{min}, w_{max}]\} \tag{6}$$

What's more, because the unmanned vehicle is affected by the motor performance, due to the limited torque of the motor, there is a maximum acceleration and deceleration limit. Therefore, the unmanned vehicle has a dynamic range within a certain simulation

period, which is the speed range of the unmanned vehicle. While (v, w) is the actual speed that unmanned vehicles can achieve:

$$V_a = \left\{(v,w) \middle| \begin{matrix} v \in [v_c - \dot{v}_d \Delta t, v_c + \dot{v}_a \Delta t], \\ w \in [w_c - \dot{w}_d \Delta t, w_c + \dot{w}_a \Delta t] \end{matrix}\right\} \quad (7)$$

Then, in order to be able to stop before hitting an obstacle, the speed must be set within a certain range under the maximum deceleration condition.

$$\begin{cases} V_\alpha = \{(v,w) | v \le \Omega\} \\ \Omega = \min\left(\sqrt{2dist(v,w)\dot{v}_d}, \sqrt{2dist(v,w)\dot{w}_d}, \left|\frac{v_r tan\alpha_{lim}}{l}\right|\right) \end{cases} \quad (8)$$

Secondly, the obstacle avoidance algorithm is designed in the path planning. There are two types of obstacles in the motion process of vehicle. One is static environmental obstacles, and the other type is other vehicles in the motion process.

Finally, the scope of the vehicle's velocity is a combination of those three equations:

$$V = V_m \wedge V_a \wedge V_\alpha \quad (9)$$

This forms the dynamic window constraint as Figure 3 shows.

The artificial potential field method [16] proposed by Khatlib is one of the commonly used methods for local online obstacle avoidance of mobile robots. Its principle is as follows:

The mobile robot moves in a virtual force field. The obstacle is surrounded by the repulsive potential field U_r. The resulting repulsive force increases with the reduction of the distance between the robot and the obstacle, and the direction deviates from the obstacle. The target point is surrounded by the gravitational potential field U_aThe resulting gravitational force decreases as the robot approaches, and the direction points to the target point. Then, according to the sum of the artificial potential energy generated by each obstacle and the target, the gradient direction of the potential function is taken to achieve collision-free path planning.

However, because the planning of the path only based on the information about the robot, obstacles and targets, the scope of its application is limited to static environments. The following modifications to the traditional artificial potential field method can make it not only track and avoid mobile obstacles but also to take the advantages of simplicity and high speed of the control system.

To achieve that, the method for calculating the radius of the repulsion circle of the original artificial potential field is combined with the relative velocity of the vehicle, and the detection range of the vehicle is ρ_0. For the ith obstacle in the ρ_0 range, the repulsive force is defined as a circle centered on the ith obstacle and a radius ρ_i, the radius of the repulsive circle is related to the relative velocity of the ith obstacle:

$$\rho_i = \left(1 + \frac{v'}{|v_{max}|}\right)\rho_r \quad (10)$$

Taking the unmanned vehicle 1 as the research object, set its own detection radius to be ρ_0. Through the perception of the surrounding environment by the unmanned vehicle, the nearest unmanned vehicle i is determined as an obstacle, and the radius of the repulsive circle is set to ρ_i

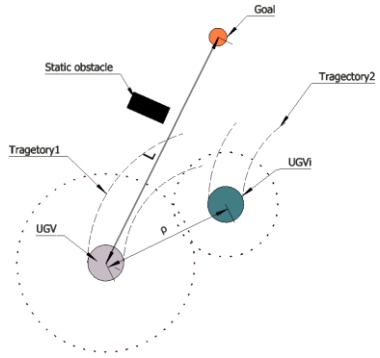

Fig.4. Potential energy field diagram

For the case of $\rho \ge \rho_i$, the vehicle did not detect obstacles, but according to previous experimental results, this would make the vehicle operationally confusing, that is, it may generate in situ circling behavior. Therefore, path planning is reconsidered in this case. First, constructing simultaneous equations that turn to the target points. Simultaneous unmanned vehicle points to the target point linear equation L(x, y) and other unmanned vehicle's repulsive force equation f(x, y) which is closest to the unmanned vehicle.

Discuss the number of roots.

1. If the function L(x, y) and the repulsive force equation f(x, y) have no roots, the vehicle does not do obstacle avoidance actions and goes directly to the target.
2. If the function L(x, y) and the repulsive force equation f(x, y) have two roots, then select the intersection point closer to the robot, make a tangent of the repulsion loop, and select the direction of the tangent toward the target, so as to process moderate preventive obstacle avoidance;
3. If L(x, y) and the repulsive force equation f(x, y) have more than three roots, do the tangent line between the robot and each effective repulsion circle, select the direction toward the robot, and determine the angle between each tangent line and L, and take the direction of the tangent with the minimum angle of L as the robot's motion direction.

On the other hand, for $\rho \le \rho_i$, using the correction formula combined with the target motion speed of the vehicle. It can be calculated:

Gravitational field potential energy function is

$$U_{att} = \frac{1}{2}K_{aq}\left|q - q_{goal}\right|^2 + \frac{1}{2}K_{av}\left|v - v_{goal}\right|^2 \quad (11)$$

The attraction function is

$$F_{att} = -grad(U_{att}) = -K_{aq}|q - q_{goal}| - K_{av}|v - v_{goal}| \quad (12)$$

The repulsive field potential energy function is

$$U_{rep} = K_{rq}[\frac{1}{\rho(q,q_{obs})} - \frac{1}{\rho_i}]^2 + K_{rv}|v_{obs} - v|^2 \quad (13)$$

The repulsive force function is

$$F_{rep} = -grad(U_{rep})$$

$$F_{rep} = K_{rq}\left[\frac{1}{\rho(q,q_{obs})} - \frac{1}{\rho_i}\right]\frac{1}{\rho(q,q_{obs})^2} \times \partial\rho(q,q_{obs}) - K_{rv}|v_{obs} - v| \quad (14)$$

This method separates the obstacles to make the obstacle avoidance action more reasonable, and at the same time introduces preventative obstacle avoidance, instead of simple and direct obstacle avoidance treatment, which can effectively assist the potential field method to complete obstacle avoidance and tracking task.

Path Tracking

Taking the center of mass of the main vehicle as the original point, the direction of the actual speed of the main vehicle as the Y-axis to set up the first coordinate system xoy. Taking the center of mass of the subordinate vehicle as the original point, the direction of the actual speed of the subordinate vehicle as the y' axis to set up the second coordinate system $x'o'y'$, as the Figure 5 shows.

When the team of vehicles is transforming the formation, each vehicle travels on its corresponding path baseline and the target path between the two routes baselines can be obtained from the aforementioned path planning method:

$$R_{ideal}(t_i) = (x_{ideal}(t_i), y_{ideal}(t_i)) \quad (15)$$

Simultaneously, the ideal velocity can be calculated as:

$$v_{ideal}(t_i) = \nabla R_{ideal}(t_i) = \begin{bmatrix} \dot{x}_{ideal}(t_i) \\ \dot{y}_{ideal}(t_i) \end{bmatrix} = \begin{bmatrix} v_x(t_i) \\ v_y(t_i) \end{bmatrix} \quad (16)$$

Currently, the speed of x, y is the first coordinate system speed.

Furthermore, calculating the expected transverse angular velocity as:

$$\omega_{ideal}(t_i) = \frac{\Delta\theta_{ideal}(t_i)}{\Delta t} = \frac{\theta_{ideal}(t_i) - \theta_{ideal}(t_{i-1})}{\Delta t} \quad (17)$$

Within the same time, the actual speed and the actual yaw angular velocity can be obtained.

The yaw angular velocity takes clockwise as positive, counterclockwise are negative.

There are three states existing when the vehicle is running on the expected path closely:

1) The vehicle is on the left side of the path.

2) The vehicle is on the right side of the path.

3) The vehicle is precisely on the path.

The three states are illustrated in the Figure 6.

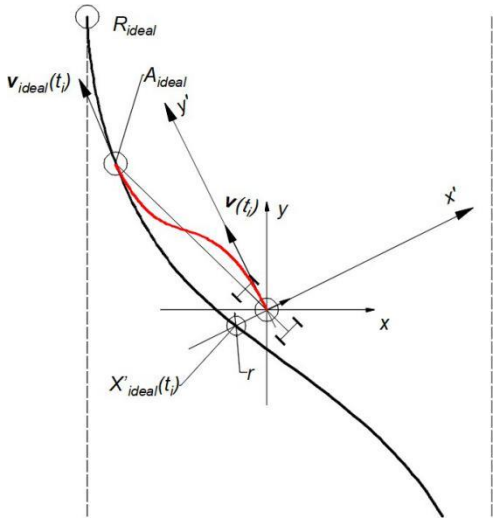

Fig.5. Hermite curve path planning for vehicles outside the expected path

Intersection the target route with the second coordinate system:

$$\begin{cases} \dot{x}_{ideal}(t_i) > 0, \textit{the vehicle is on the left side of the path} \\ \dot{x}_{ideal}(t_i) < 0, \textit{the vehicle is on the right side of the path} \\ \dot{x}_{ideal}(t_i) = 0, \text{the vehicle is precisely on the path} \end{cases} \quad (18)$$

With respect to the third case, it is obvious that the case is too ideal to come across. Therefore, to make the model more practical, this paper just defines a circle whose base point is the center of mass of the vehicle and its radius is relatively small, and when the path has an intersection with the circle; it is regarded as the vehicle on the path. Then the third case is converted to be:

$$\begin{cases} x'_{ideal}(t_i) > 0, \text{the vehicle is on the left side of the path} \\ x'_{ideal}(t_i) < 0, \text{the vehicle is on the right side of the path} \\ |x'_{ideal}(t_i)| - r < 0, \text{the vehicle is on the path} \end{cases} \tag{19}$$

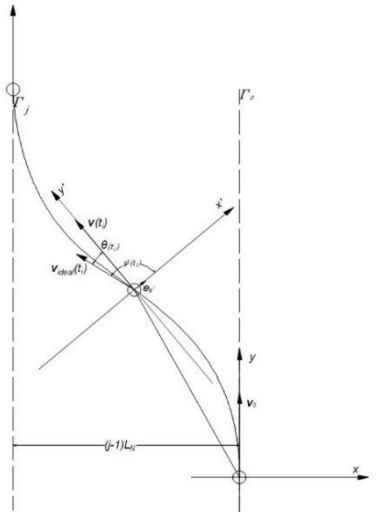

Fig.6.state judgment when the vehicle is running on the expected path

When the centroid of the vehicle deviates from the desired trajectory, extend the axis of the vehicle and intersect the desired path $R_{ideal}(t_I)$ at point A_{ideal} .

The magnitude and direction of the speed and yaw rate at this point can be calculated using the method in 2.1. The position is shown in the Figure 5.

At the same time, the coordinates of the current position of the vehicles and the direction of the actual speed are known. Considering that the vehicle is traveling, not only it is necessary to reach a predetermined position, but also it is necessary to set the front of the vehicle in the process so as to facilitate the next driving. Therefore, the path should meet the following conditions: 1) smooth transition; 2) starting point and arrival point are on this path; 3) initial velocity vector and key velocity vector are tangent to this path (right front). About the three conditions, it was found that parameterized curve Hermite curve could meet the condition 1). The parameters of the Hermite curve are set up according to the constraints of the starting point and the terminal coordinates and the velocity vector.

$$\boldsymbol{p}(u) = \boldsymbol{a}u^3 + \boldsymbol{b}u^2 + \boldsymbol{c}u + \boldsymbol{d} \quad 0 \le u \le 1 \tag{20}$$

$$\begin{cases} \mathbf{a} = 2\mathbf{p}_0 - 2\mathbf{p}_1 + \mathbf{p}_0^u + \mathbf{p}_1^u \\ \mathbf{b} = -3\mathbf{p}_0 + 3\mathbf{p}_1 - 2\mathbf{p}_0^u - \mathbf{p}_1^u \\ \mathbf{c} = \mathbf{p}_0^u \\ \mathbf{d} = \mathbf{p}_0 \end{cases} \tag{21}$$

In the formula(19),p_0, p_1 is the current point and the coordinate of point A_{ideal} , p_0^u p_1^u is the velocity vector of the current point and the point A_{ideal} .

Using this curve to plan a new approach trajectory, the problem of the vehicle's deviation from the original path tracking is converted into a new vehicle's path tracking, while for the new path tracking method, a tracking method of a vehicle on a path to be described later can be used

When the vehicle's centroid is on the desired trajectory, a vector tracking method [2] is used to model the vehicle-tracking path.

Calculate the angle between the actual speed and the expected speed of the vehicle during formation change, as shown in Figure 5.

$$\theta(t_i) = \arccos\left(\frac{\boldsymbol{v}(t_i)\cdot\boldsymbol{v}_{ideal}(t_i)}{|\boldsymbol{v}(t_i)||\boldsymbol{v}_{ideal}(t_i)|}\right) \tag{22}$$

Calculate the cosine of angle between the expected direction of velocity and the x' -axis of the second coordinate system:

$$\psi(t_i) = \cos(\varepsilon(t_i)) = \frac{\boldsymbol{e}_{x'}\cdot\boldsymbol{v}_{ideal}(t_i)}{|\boldsymbol{e}_{x'}||\boldsymbol{v}_{ideal}(t_i)|} \tag{23}$$

In this formula,$e_{x'}$ is the unit vector of x-axis.

Setting the angle threshold $\theta_{threshold}$,

$$\begin{cases} \psi(t_i) \ge 0, \text{the subordinate vehicle needs to turn right} \\ \psi(t_i) < 0, \text{the subordinate vehicle needs to turn left} \end{cases} \tag{24}$$

Then the Steering determination formula is:

$$\varphi(t_i) = \max(\theta(t_i) - \theta_{threshold}, 0)\cdot\psi(t_i) \tag{25}$$

Set speed threshold $v_{threshold}$, judgment conditi speed adjustment

$$f(t_i) = \max\left(\left||\boldsymbol{v}_{ideal}(t_i)| - |\boldsymbol{v}(t_i)|\right| - v_{threshold}, 0\right)\cdot\left(|\boldsymbol{v}_{ideal}(t_i)| - |\boldsymbol{v}(t_i)|\right) \tag{26}$$

$$\begin{cases} f(t_i) > 0, \text{the subordinate vehicle needs to accelerate} \\ f(t_i) = 0, \text{the subordinate vehicle needs to maintain the orginal speed} \\ f(t_i) < 0, \textit{the subordinate vehicle needs to decelerate} \end{cases} \tag{27}$$

The adjustment model is

$$\begin{cases} \boldsymbol{v}(t_{i+1}) = \boldsymbol{v}(t_i) + sign\big(f(t_i)\big) \cdot \frac{|v_{ideal}(t_i)| - |v(t_i)|}{\tau} \\ \boldsymbol{\omega}(t_{i+1}) = \boldsymbol{\omega}(t_i) + sign\big(f(t_i)\big) \cdot \frac{\theta(t_i) - \theta_{threshold}}{\tau} \end{cases} \tag{28}$$

In the process of turning adjustment of the vehicle, the change of speed and yaw rate should be uniform and stable, to avoid instability in turn, the vehicle rollover and so on.

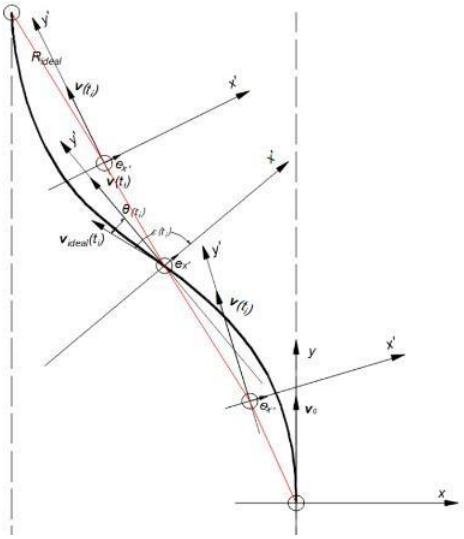

Fig.7. following coordinates establishing the relative position between the vehicle and the expected path

Experiment and Performance Evaluation

The structure of the formation system

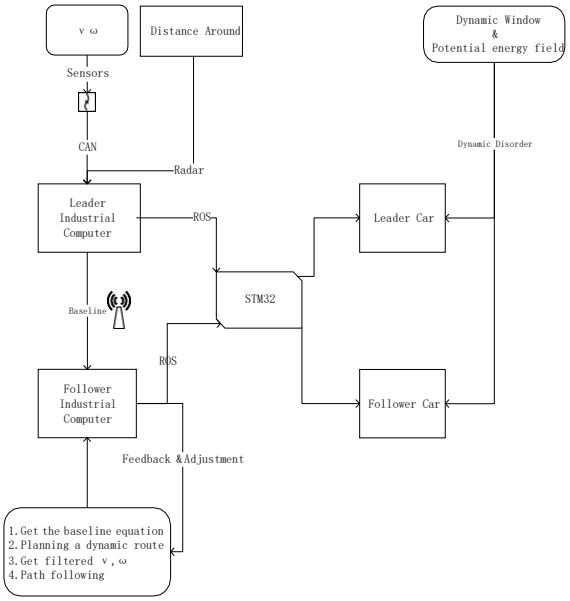

Fig .8. Formation System Architecture

The formation system consists of hardware part and software part. The hardware part includes the main portion of the main and subordinate cars, industrial computers, STM32 microcontrollers, and a series of sensors onboard the vehicle. The software part includes the portion of path planning and path tracking of combination of the dynamic window approach and potential energy field. In the running process, the master car and the slave cars communicate via WiFi. The master car transmits the baseline equation of its own path to the corresponding slave cars through offset transformation. After receiving the signal of baseline equation from the vehicle, the path planning method is used to obtain an optimal path to the baseline. At the same time, the vehicle speed and yaw rate collected by the on-board sensors are filtered and used as input, then utilizing the path tracking method, the program is burned into the MCU through the IPC to achieve the aforementioned formation transformation.

Simulation in ROS

ROS(Robot Operating System, the abbreviation is "ROS" in the following section)[27] is an open source meta-operating system suitable for robots. It provides the services that an operating system should have, including hardware abstraction, low-level system control, implementation of common functions, inter-process messaging, and package management. It also provides the tools and library functions which are required to obtain, compile, write, and operate codes across computers. ROS is a distributed process (that is, the "node") framework, which is encapsulated in packages and functional packages that are easy to be shared and released. All projects can be integrated by the basic tools of ROS. The actual robot can be moved by the software package compiled in the system. Based on the ROS robot operating system, this paper simulates the formation control of five unmanned vehicles, and the simulation results can be used to verify the implement ability of the controller. [28]

As shown in the aforementioned formation process, setting the simulation process resolution to 0.02, which is calculated every 0.02s. .Firstly, the initial state is the formation A, which is, along the longitudinal line, the vehicle formation transform to the middle state B, which is a skew formation, by issuing a command to convert the formation. The transmitting time is 11.6s, and the relative positions can be regulated by the adjustment of the relative velocity so that the skew formation can be transformed into a horizontal line and the transmitting time is 3s; and then, following the same steps to adjust the relative positions in order to convert the formation to a triangular one.

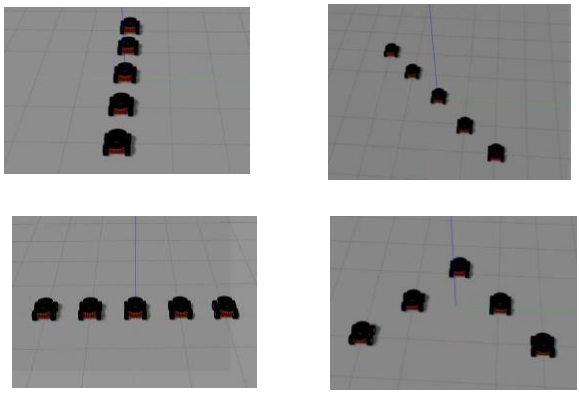

Fig .9. The test of formation transforming

Result Analysis

There are three main aspects to evaluate the performance of a control system: under the control of the system, the proximity of the vehicle's real time position to the theoretical position, the close degree of the actual speed of the vehicle to the expected speed, and the fluctuation of the speed of the vehicle, that is, the magnitude of the acceleration. In accordance with the above three criteria, a proper weight is set for each of them, and then constructs the control index function W, which could be used to evaluate the control performance of the control system, and the functional relation is as follows:

$$W = \int_0^{\infty} \left[(s(t) - s_{ideal}(t))^2 + 9 \times \left(\frac{v(t) - v_{ideal}(t)}{3.6} \right)^2 + 25 \times (a(t))^2 \right] dt \qquad (29)$$

The smaller the W value is, the better function that the control system possesses. According to the control index function W, it could be found that the best control strategy to track the target path under the condition of slight acceleration fluctuation.

In the design simulation experiment, a planned lane change path

$$R_{ideal}(t_i) = \left(x_{ideal}(t_i), y_{ideal}(t_i) \right) \qquad (30)$$

is obtained first, and the path is deduced with respect to time, and the change of the line speed of the whole path is obtained. In this case, the speed change is the ideal speed curve, and the ideal speed direction is the tangent of the ideal path at the corresponding position.

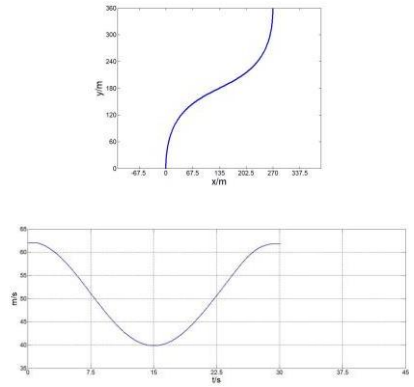

Fig.10. path diagram and speed transformation diagram corresponding to the path

Adopting the above-mentioned control strategy, the results of simulation as follows

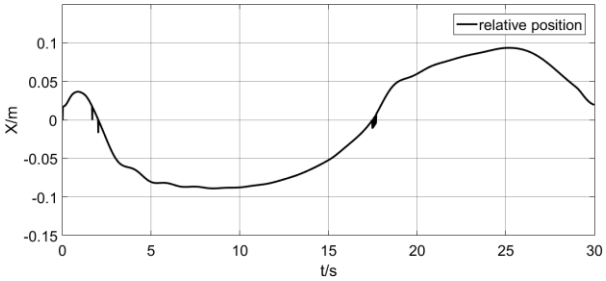

Fig.11. Simulation result of longitudinal error

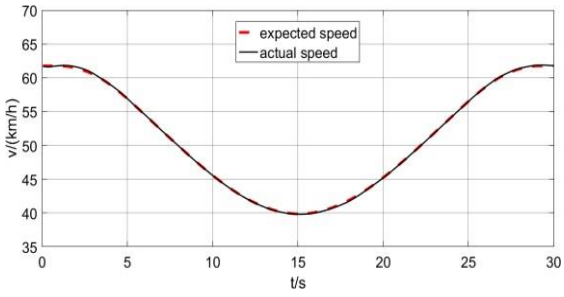

Fig.12. Simulation result of the expected speed and the actual speed

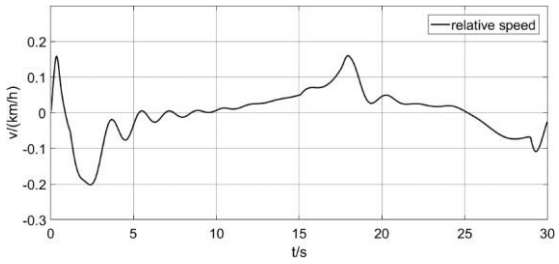

Fig.13. Simulation result of speed error

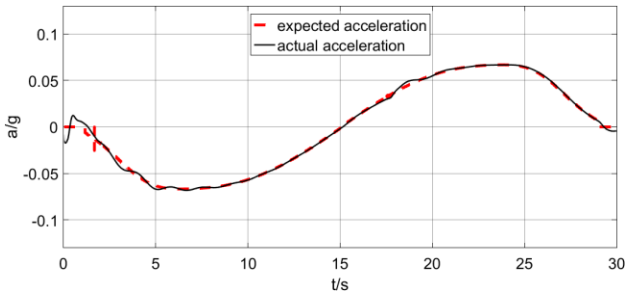

Fig.14. Simulation result of the expected acceleration and the actual acceleration

Analysis of the above figures:

The relative position in Figure 11 is the difference between the actual position of the vehicle and the desired position. Under the control system, the vehicle can track the change of the desired position very rapidly; the maximum error is about 0.1 meters in the whole process, which reflects high tracking accuracy.

In Figure 12, the dotted line is the desired vehicle speed and the solid line is the actual vehicle speed. When the desired speed changes rapidly, the self-vehicle speed can respond in time and the overshoot is relatively inconspicuous. When the desired vehicle speed is keeping constant, the self-vehicle can follow at a stable vehicle speed without generating oscillation, which reflects the system is relatively stable.

In Figure 13, the relative speed is the difference between the actual vehicle speed and the desired vehicle speed. The simulation shows that the speed error can be controlled within 0.2km/h. Within 0-5s, the vehicle just enters the path tracking state, the speed fluctuates greatly, and fluctuation of the rate is obvious. Within 5-25 seconds, the vehicle is in a stable path tracking state, and the vehicle speed has a relatively high stability. 25-30s, the lane change is completed, and the speed is slightly fluctuating. It can be seen from the figure 12 that the vehicle has high stability at low speed, while the speed is fluctuating when driving at high speed.

In Figure 14, the maximum acceleration a_{max} = 0.07g, indicating that under the control system, the speed of the vehicle changes smoothly, and there is no dangerous condition of rapid acceleration and rapid deceleration, which is beneficial to improve driving safety.

Summary and Conclusion

This paper introduces a relatively new method of dynamic planning path and path following of unmanned vehicles, proposes a collaborative formation controller design for multiple unmanned ground vehicles designs from two aspects as path planning and path following. Finally, the simulation is performed in accordance with the design.

In the aspect of path planning, the DWA algorithm can effectively avoid static obstacles, but when vehicles encounter the dynamic obstacles, they will move along with the obstacles, which will develop great disturbance to the path planning. Therefore, this paper adopts the obstacle avoidance algorithm based on dynamic window approach and potential energy field method, which effectively reduces the possibility of interference caused by other platform movements during the process of changing teams. It also enables vehicles to track the movement of the target point more fleetly and precisely. In the meanwhile, through a series of constraints based on the vehicle's own performance, the vehicle can avoid rapid acceleration or deceleration, meaning this new approach has good maneuverability.

In the aspect of path tracking, due to considering some specific vehicles formation situations, this paper reduces the motion control to the speed of the vehicle and the yaw rate, and then the baseline equation, which is calculated by the path planning algorithm, is transmitted from the main vehicle to the subordinate vehicle. After that, the state decision function and the state adjustment function is set; the former controls the steering direction, acceleration and deceleration of the vehicle while the latter controls the regulation of the speed based on the time. When the vehicle deviates from the expected path, the algorithm extends the axis of the vehicle and gets an intersection with the path. Based on the intersection and its expected speed, its current position and speed, planning a smooth Hermite curve not only to ensure that the vehicle is able to approach the original well planed path smoothly, but also to fix the direction of the vehicle's headstock in the process.

Finally, the control performance of the path following control system is verified by simulation experiments in this paper. Throughout the simulation process, the vehicle can track the variation of the expected position fleetly and precisely, with a maximum error of 0.1m, and in the meanwhile, the vehicle can follow the expected speed rapidly with an inconspicuous overshoot, and the speed error can be controlled within 0.2km/h. Therefore, the path tracking control system guarantees the formation stability of multiple unmanned vehicles.

Despite all these achievements, there are still several aspects able to be improved. One is that the parameter curves in the path tracking will become tortuous because of the transition process, when the initial velocity is large and the distance is close, and the void displacement will decrease the efficiency of the algorithm. Therefore, how to set the speed of the end position of the path in the planning process requires in-depth consideration. The next aspect worth considering is that in the formation process, the path planning method proposed in this paper only takes two kinds of variables into account, which is the other moving vehicles and obstacles in the map. In the future, the dynamic obstacles of the unknown motion trajectory can be added to the system, as another variable to test the system's ability to adapt to such obstacles. In this paper, the parameters of vehicle

size and centroid height are not deeply studied. If the limitation of the vehicle's own parameters is added to the path planning, the formation of small-pitch formation can be realized. This problem also requires in-depth consideration.

Acknowledgements

The authors gratefully thank the reviewers for their valuable suggestions and the finial support from CoolHigh Tech(Beijing) Co,Ltd.

Reference

[1] Gage, D. W. (1995). Ugv history 101: a brief history of unmanned ground vehicle (ugv) development efforts. *Unmanned Systems, 13*, 9-32.

[2] Iii, C. D. C., Ii, D. G. A., Touchton, R., Galluzzo, T., Solanki, S., & Lee, J., et al. (2010). Team cimar's navigator: an unmanned ground vehicle for the 2005 darpa grand challenge. *Journal of Field Robotics, 23*(8), 599-623.

[3] Wells, P. (2005). Talon: a universal unmanned ground vehicle platform, enabling the mission to be the focus. *Proceedings of SPIE - The International Society for Optical Engineering, 5804*.

[4] Burgard, W., Moors, M., Stachniss, C., & Schneider, F. E. (2005). Coordinated multi-robot exploration. *IEEE Transactions on Robotics,21*(3), 376-386.

[5] Olson, E., Strom, J., Morton, R., Richardson, A., Ranganathan, P., & Goeddel, R., et al. (2012). Progress toward multi-robot reconnaissance and the magic 2010 competition. *Journal of Field Robotics, 29*(5), 762-792.

[6] Yanco, H. A., & Drury, J. L. (2007). Rescuing interfaces: a multi-year study of human-robot interaction at the aaai robot rescue competition. *Autonomous Robots, 22*(4), 333-352.

[7] Cong, M., & Fang, B. (2008). Multisensor fusion and navigation for robot mower. *IEEE International Conference on Robotics and Biomimetics*(pp.417-422). IEEE.

[8] Nikitenko, A., Grundspenkis, J., Liekna, A., Ekmanis, M., Kulikovskis, G., & Andersone, I. (2014). Multi-robot System for Vacuum Cleaning Domain. *Paams International Conference on Practical Applications of Agents and Multi-Agent Systems* (Vol.8473, pp.363-366).

[9] Allard, J., Barrett, D. S., Filippov, M., Pack, R. T., & Svendsen, S. (2009). Systems and methods for control of an unmanned ground vehicle. *US, US 7499776 B2*.

[10] Borhaug, E., Pettersen, K. Y., & Pavlov, A. (2006). An optimal guidance scheme for cross-track control of underactuated underwater vehicles. *Mediterranean Conference on Control and Automation* (pp.1-5). IEEE.

[11] Wei, R., & Sorensen, N. (2008). Distributed coordination architecture for multi-robot formation control. *Robotics & Autonomous Systems, 56*(4), 324-333.

[12] Li, X., & Xiao, J. (2005). Robot formation control in leader-follower motion using direct lyapunov method. *International Journal of Intelligent Control & Systems*.

[13] Lewis, M. A., & Tan, K. H. (1997). High precision formation control of mobile robots using virtual structures. *Autonomous Robots, 4*(4), 387-403.

[14] Balch, T., & Arkin, R. C. (1999). Behavior-based formation control for multirobot teams. *IEEE Transactions on Robotics & Automation, 14*(6), 926-939.

[15] Mas, I., & Kitts, C. (2010). Centralized and decentralized multi-robot control methods using the cluster space control framework. *Ieee/asme International Conference on Advanced Intelligent Mechatronics* (Vol.58, pp.115-122).

[16] Min, C. L., & Min, G. P. (2003). *Artificial potential field based path planning for mobile robots using a virtual obstacle concept*.

[17] Jeff Wit, Carl D. Crane III, & David Armstrong. (2010). Autonomous ground vehicle path tracking. Journal of Field Robotics, 21(8), 439–449.

[18] Heredia, G. (2002). Stability analysis of mobile robot path tracking. Ieee/rsj International Conference on Intelligent Robots and Systems 95. 'human Robot Interaction and Cooperative Robots', Proceedings (Vol.3, pp.461-466 vol.3). IEEE.

[19] Koh, K. C., & Cho, H. S. (1999). A smooth path tracking algorithm for wheeled mobile robots with dynamic constraints. Journal of Intelligent & Robotic Systems, 24(4), 367-385.

[20] Kanayama, Y., Kimura, Y., Miyazaki, F., & Noguchi, T. (1991). A stable tracking control method for an autonomous mobile robot. IEEE International Conference on Robotics and Automation, 1990. Proceedings (Vol.1, pp.384-389 vol.1). IEEE Xplore.

[21] Wang,Yan Qing, Ye,Yan Hui, & Zhang,Hua. (2011). A stable tracking control method for an autonomous welding mobile robot. Applied Mechanics & Materials, 79, 264-269.

[22] University, S., & Ji, N. (2007). Shape interpolating geometric g~1 hermite curves. Journal of Computer-Aided Design & Computer Graphics.

[23] Jeff Wit, Carl D. Crane III, & David Armstrong. (2010). Autonomous ground vehicle path tracking. Journal of Field Robotics, 21(8), 439–449.

[24] Piserchia, G. T., & Wilson, E. F. (1994). Vehicle guidance track system. US, US5297484.

[25] Cookeyarborough, R. E. (1964). Critical path planning and scheduling: an introduction and example. *Review of Marketing & Agricultural Economics,32*(01).

[26] Min, C. L., & Min, G. P. (2003). Artificial potential field based path planning for mobile robots using a virtual obstacle concept. *Ieee/asme International Conference on Advanced Intelligent Mechatronics, 2003. Aim 2003. Proceedings* (Vol.2, pp.735-740 vol.2). IEEE.

[27] Kim, J., & Jung, S. (2002). A Dynamic Window-Based Approximate Shortest Path Re-computation Method for Digital Road Map Databases in Mobile Environments. *Eurasian Conference on Information and Communication Technology* (Vol.2510, pp.711-720). Spcircleer-Verlag.

[28] Quigley, M. (2009). ROS : an open-source Robot Operating System. Proc. IEEE ICRA Workshop on Open Source Robotics (Vol.3).